CONF-760822--4

EXPERIMENTAL STUDIES ON THE KRYPTON ABSORPTION IN LIQUID CO_2 (KALC) PROCESS*

R. W. Glass, H. W. R. Beaujean,** V. L. Fowler, T. M. Gilliam,
D. J. Inman, and D. M. Levins***

Oak Ridge National Laboratory
Oak Ridge, Tennessee

For presentation at the 14th ERDA Air Cleaning Conference to be held in Sun Valley, Idaho, August 1-4, 1976.

---

[*] Research sponsored by the [redacted]. Energy Research and Development Administration under contract with Union Carbide Corporation Nuclear Division.

[**] Guest scientist from West Germany. Present address: Institute for Chemische Technologie, der Kernforschungsanlage, Julich GmbH, 517 Julich, West Germany.

[***] Guest scientist from Australia. Present address: Chemical Technology Division, Australian Atomic Energy Commission, Research Establishment, Private Mailbag, Sutherland 2232, N.S.W. Australia.

EXPERIMENTAL STUDIES ON THE KRYPTON ABSORPTION IN LIQUID CO_2 (KALC) PROCESS*

R. W. Glass, H. W. R. Beaujean,** V. L. Fowler, T. M. Gilliam,
D. J. Inman, and D. M. Levins***

Oak Ridge National Laboratory
Oak Ridge, Tennessee

Abstract

Results are presented for a series of experiments to quantify krypton removal from simulated High-Temperature Gas-Cooled Reactor reprocessing off-gas by the KALC process. The Experimental Engineering Section Off-Gas Decontamination Facility used in the campaign provides engineering-scale experiments with nominal gas and liquid flows of 5 scfm and 0.5 gpm respectively.

Equilibrium and nonequilibrium mass transfer experiments for the CO_2-O_2-Kr system are described. Data analysis indicates values of HTU for krypton on the order of 0.5 ft for decontamination factors from 100 to 10,000. Recent flooding information for the packed columns is combined with previous data and is shown to be well represented by an empirical flooding equation.

Introduction

As part of the Thorium Utilization Program developmental work being carried out at the Oak Ridge National Laboratory, the Experimental Engineeering Section Off-Gas Decontamination Facility(1) (EES-ODF, see Fig. 1) has been operated to quantify the absorption of krypton by liquid CO_2. The work presented here comprises approximately 30 experiments involving the mass transfer of krypton into liquid CO_2 in the presence of O_2 and 10 experiments in which conditions within the packed absorption column were chosen such that CO_2-Kr equilibrium values were obtained as a check on values of equilibrium data reported in the literature.(2,3) Additional column flooding data are also presented and compared with previous values.(1)

---

*Research sponsored by the [redacted] Energy Research and Development Administration under contract with Union Carbide Corporation Nuclear Division.

**Guest scientist from West Germany. Present address: Institute for Chemische Technologie, der Kernforschungsanlage, Julich GmbH, 517 Julich, West Germany.

***Guest scientist from Australia. Present address: Chemical Technology Division, Australian Atomic Energy Commission, Research Establishment, Private Mailbag, Sutherland 2232, N.S.W. Australia.

ORNL DWG 73-3511

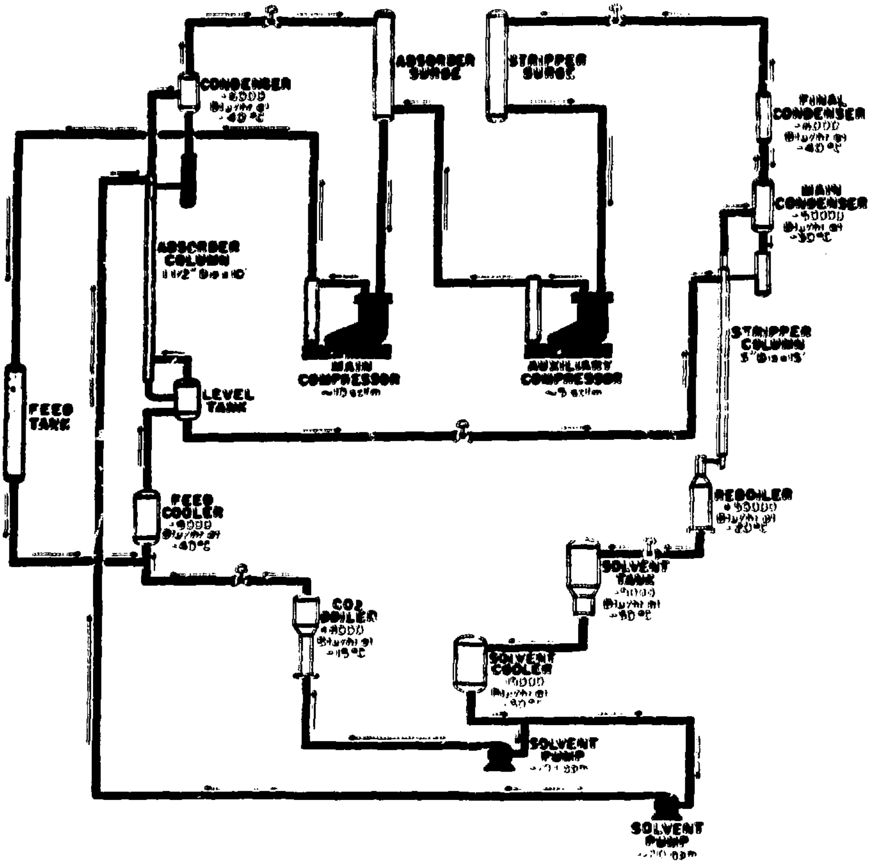

Fig. 1. Experimental Engineering Section Off-Gas Decontamination Facility.

Flooding Studies

Fluid dynamic data for the EES-ODF packed columns have been reported.(1) More recently, a few additional experiments with the liquid CO_2 system were conducted during a High-Temperature Gas-Cooled Reactor (HTGR) campaign in the Oak Ridge Gaseous Diffusion Plant (ORGDP) facility for off-gas decontamination studies.(4)

Figure 2 presents the collective flooding information obtained for the packed columns investigated. Included in the data shown in this figure are flooded conditions found for the 1-1/2-in. absorber column and the 3-in. stripper column in the EES-ODF, together with the more recent data (darkened points) acquired from operation of the 3-in. fractionator column in the ORGDP facility. All columns are packed with presized canisters (6 in. long) of Goodloe* wire mesh packing.

The flooding curve is presented in a standard form for the particular packing (i.e., no "packing factor" is included in the ordinate grouping). The following quantities are noted for Fig. 2:

L = liquid flow rate, $lb/ft^2 \cdot hr$,
G = gas flow rate, $lb/ft^2 \cdot hr$,
ρ_G = gas-phase density, lb/ft^3,
ρ_L = liquid-phase density, lb/ft^3,
μ_L = liquid-phase viscosity, cP,
U_M = gas velocity at flooding, ft/sec,
g = 32.2 ft/sec^2.

With the addition of the four experimental points from the ORGDP fractionator, a curve has been fitted to all points shown. The results are as follows:

$$\bar{y} = a + b\bar{x} + c\bar{x}^2 = \log(y), \qquad (1)$$

where

$\bar{x} = 2.0 + \log(x)$,

y = ordinate values of $\dfrac{U_M^2 \rho_G \mu_L^{0.2}}{g \rho_L}$,

x = abscissa values of $\dfrac{L}{G}\sqrt{\dfrac{\rho_G}{\rho_L}}$,

$a = -3.44748$,

$b = 0.379889$,

$c = -0.315457$.

---

[*] A product of the Packed Column Co., a Division of Metex Corp., Edison, N.J.

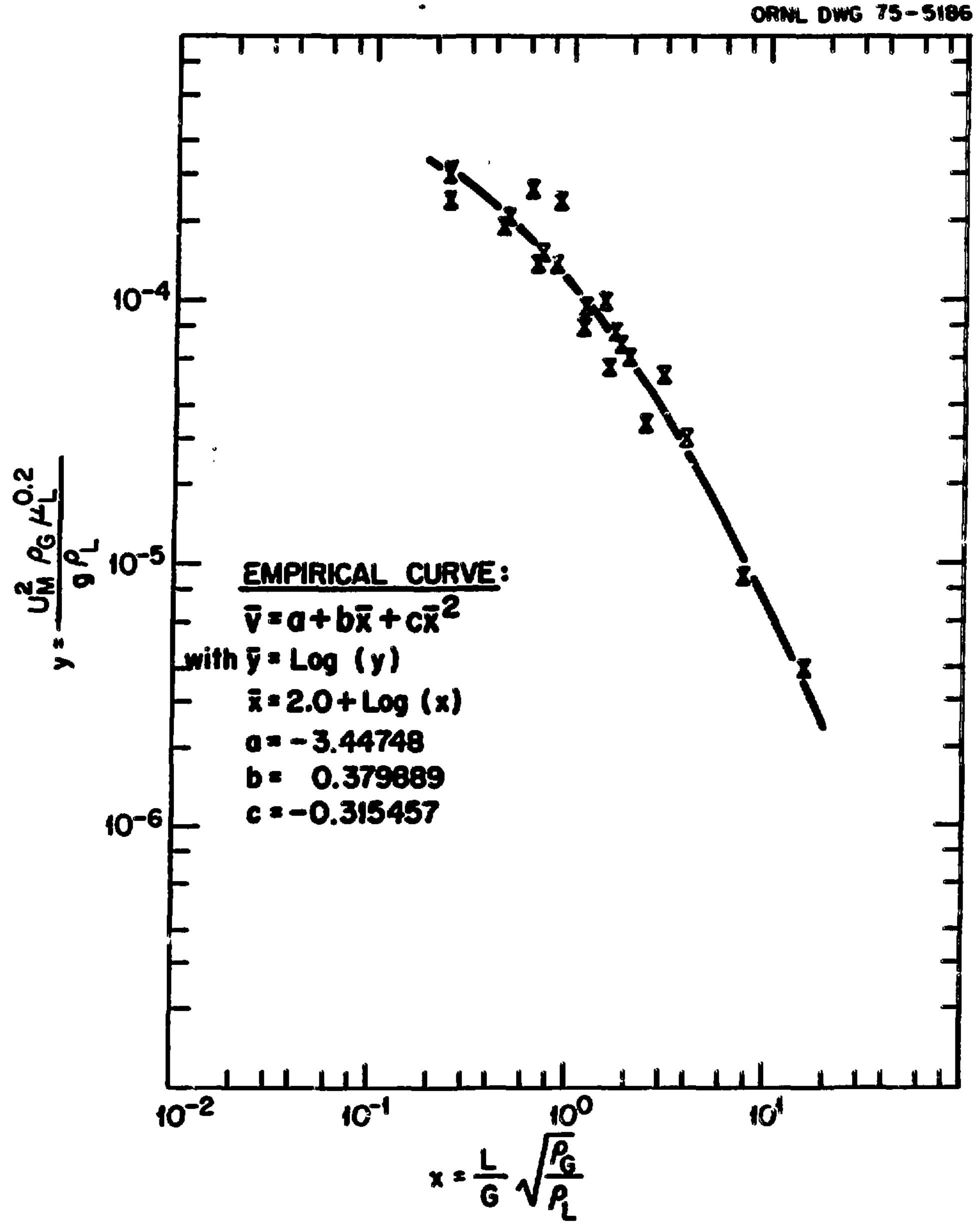

Fig. 2. Curve constructed by using collective flooding information.

Practically all of the fluid dynamic experiments represented by the flooding curve have involved CO_2 only (i.e., both gas and liquid phases are essentially pure CO_2). The effect of light gases such as O_2, N_2, etc., is not experimentally implicit. However, most of the areas of concern in the KALC process involve pure CO_2. The capacity or throughput of the packing at flooding is less than that suggested in literature supplied by the vendor (overall, by perhaps 50% depending on conditions). The pressure drop at flooding is approximately 0.5 in. H_2O per foot of packing.

Equilibrium Operations

At the beginning of the present work, it was recognized that a fundamental question concerning Kr-CO_2 equilibrium existed. The problem can be explained by referring to Fig. 3. Two independent sets of equilibrium data(2,3) for the same system were available, and these were not in agreement. The data are expressed as the equilibrium ratio y/x, where y and x denote krypton concentrations in the vapor and liquid CO_2 phases, respectively. Calculations based on each set of data produce widely varying results.(5) Moreover, decisions as to what experimental conditions to use for the present work depended on the value of the Kr-CO_2 equilibrium ratio. Thus a series of experiments was conducted early to determine whether the dilemma could be resolved.

Two important considerations are worth noting. First, the EES-ODF is not designed to provide equilibrium data <u>per se</u>. Since the facility involves equilibrium in an indirect manner, it is a question of precision regarding the worth of equilibrium observations. Second, the degree of accuracy relative to sampling and analysis is very difficult to establish, especially in limited-time operations. Consequently, the objective of the equilibrium studies was to present evidence as to which set of equilibrium data was more nearly accurate. The studies also allowed a pseudo-quantitative evaluation of sampling and analytical techniques for the EES-ODF. Details of the sampling, monitoring, and analytical techniques for the EES-ODF are presented elsewhere.(1,6)

Table 1 presents the basic data for the ten equilibrium experiments. The method of operation during these experiments was straightforward. The facility was operated with varying amounts of oxygen, at different pressures and temperatures, but always with the liquid-to-vapor flow ratio in the absorber column set to produce a "pinched" condition at the bottom of the packed section. A pinched condition results when the liquid-to-vapor ratio is less than the equilibrium ratio (y/x), given sufficient packed section length. The result of operating in a pinched mode is that the vapor entering and the liquid leaving the column will be essentially in equilibrium.

Table 2 summarizes the equilibrium experiments with regard to the facility method of operation. After sufficient time had been allowed for system transients to subside in each run, both the gas and the liquid at the bottom of the packed section were sampled and analyzed for krypton and O_2. Calculated values given in Table 1 are based on the CO_2-O_2-Kr equilibrium model described in ORNL/TM-4947.(7) The equilibrium model assumes the validity of the data of Notz et al.(3) for krypton. Figures 4 and 5 present the computer model results for the equilibrium ratio and Henry's constant for the various components.

Figure 6 presents summary results of the equilibrium studies. Values of y and x (mole fraction) for krypton were determined by sampling and analysis, and

ORNL DWG 72-6887R5

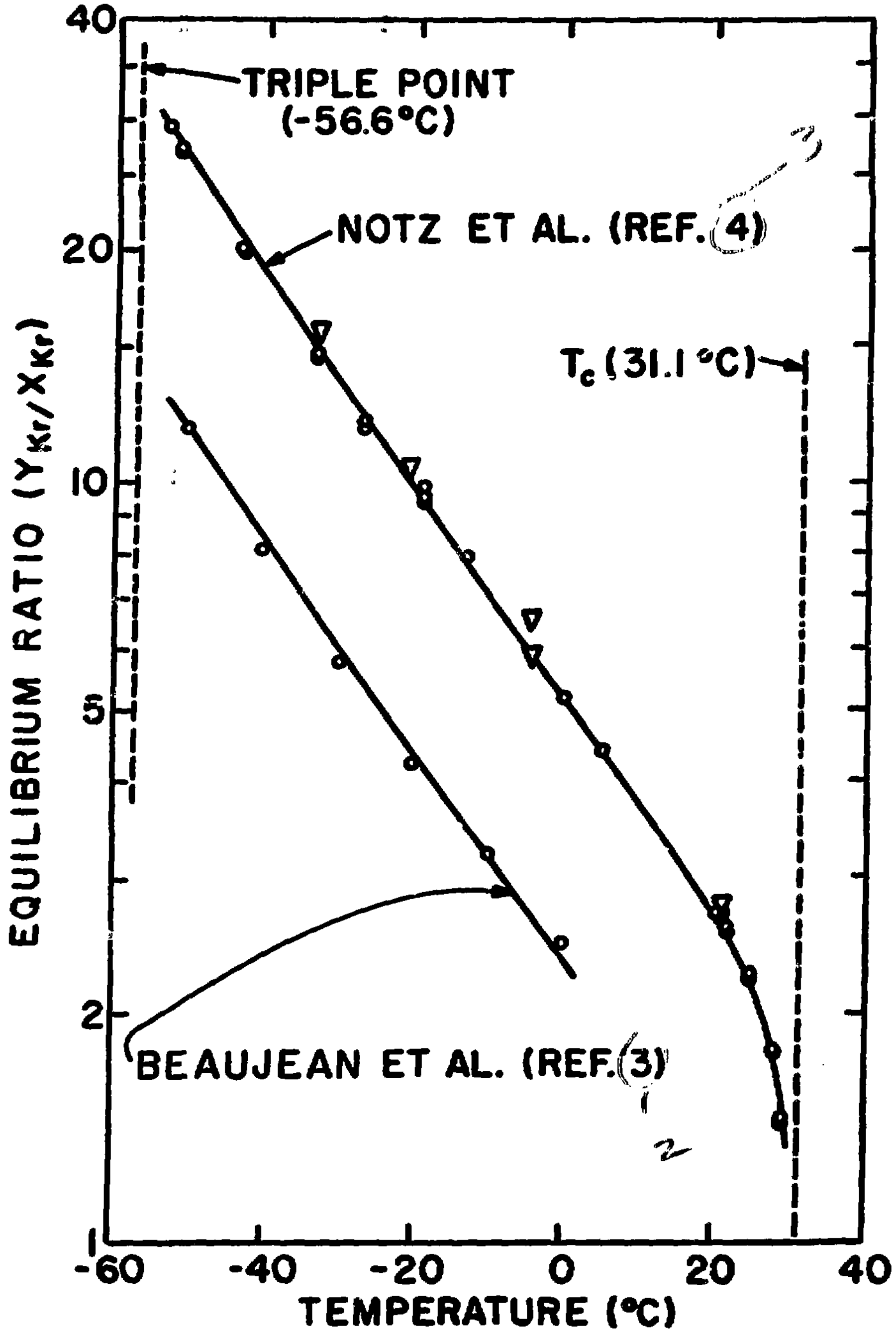

Fig. 3. Comparison of Kr-CO_2 equilibrium ratios from two independent sources.

Table 1. Summary of results obtained in ten equilibrium experiments in the EES-ODF

Experiment number	Pressure (psig)	Temperature (°C)	y_{O_2}		$(y/x)_{Kr}$	
			Measured	Calculated[a]	Measured	Calculated[a]
232	340	-17.5	0.0770	0.1005	6.94	7.74
241	254	-28.5	0.1510	0.1537	9.02	10.23
254	375	-12.1	0.0790	0.0534	6.90	7.00
268	309	-18.5	0.0338	0.0579	8.31	8.49
275-A	338	-13.5	~0	0.0103	7.17	7.75
275-B	280	-19.6	~0	0.0130	8.72	9.33
275-C	286	-19.4	~0	0.0238	9.75	9.14
275-D	218	-27.3	~0	0.0202	11.81	11.82
275-E	290	-19.0	~0	0.0245	7.90	9.02
296	290	-25.7	(0.1180)	0.1738	8.85	9.03

[a] Calculations were based on the CO_2-Kr-O_2 model presented in ORNL-TM-4947.(7) The $(y/x)_{Kr}$ ratio was calculated assuming the validity of the data of Notz et al. (3)

Table 2. Summary of experimental equilibrium operations

Experiment number	Description of operation
232	Typical mass transfer experiment involving both gas and liquid countercurrent operation with a low value of liquid-to-vapor ratio
241	Similar to 232
254	Similar to 232
268	Similar to 232
275-A	Only liquid flow in operation; equilibrium with overgas achieved by long-term system operation
275-B	Similar to 275-A
275-C	Similar to 275-A
275-D	Similar to 275-A
275-E	Similar to 275-A
296	Similar to 232

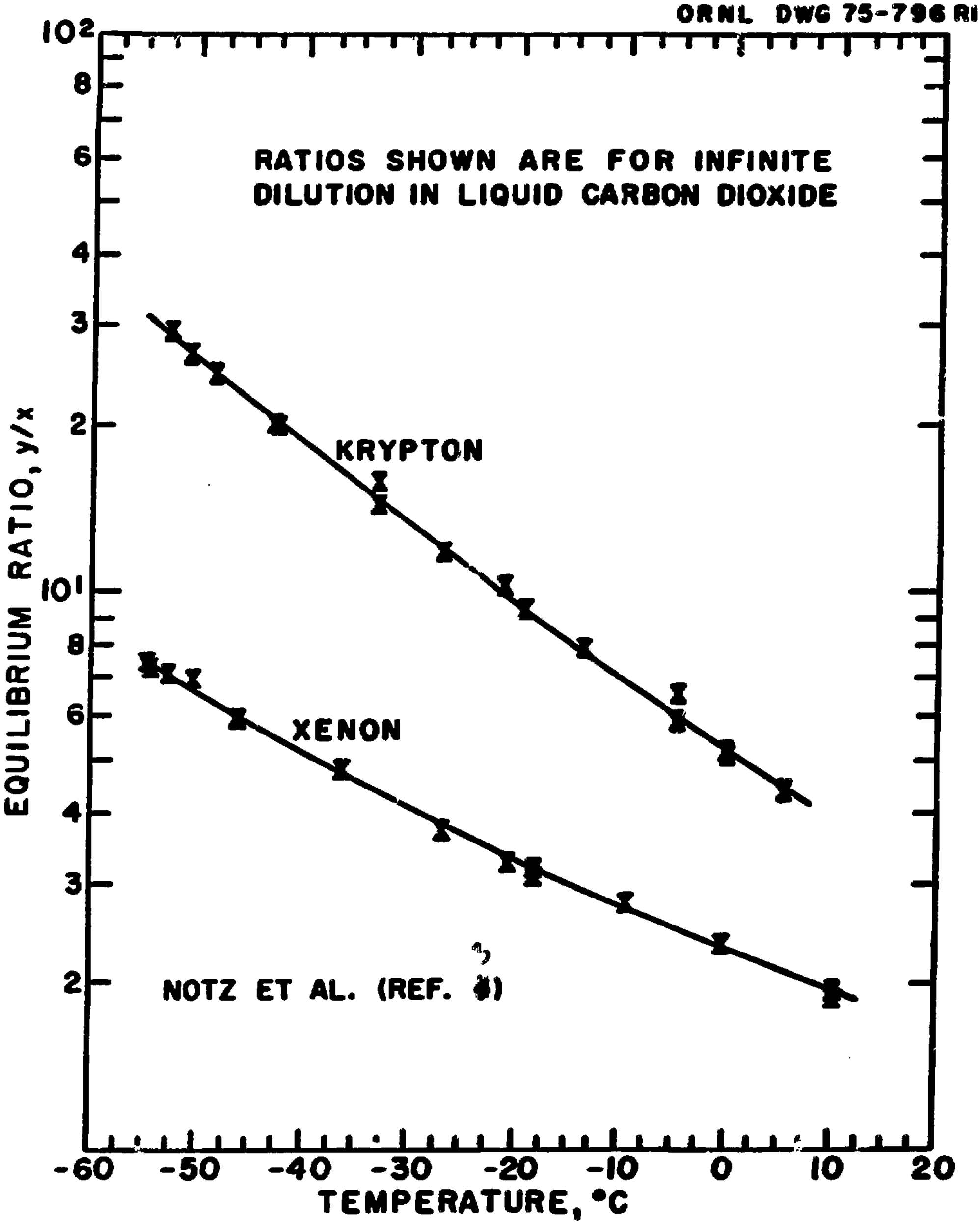

Fig. 4. Krypton and xenon equilibrium ratios as obtained by the computer model.

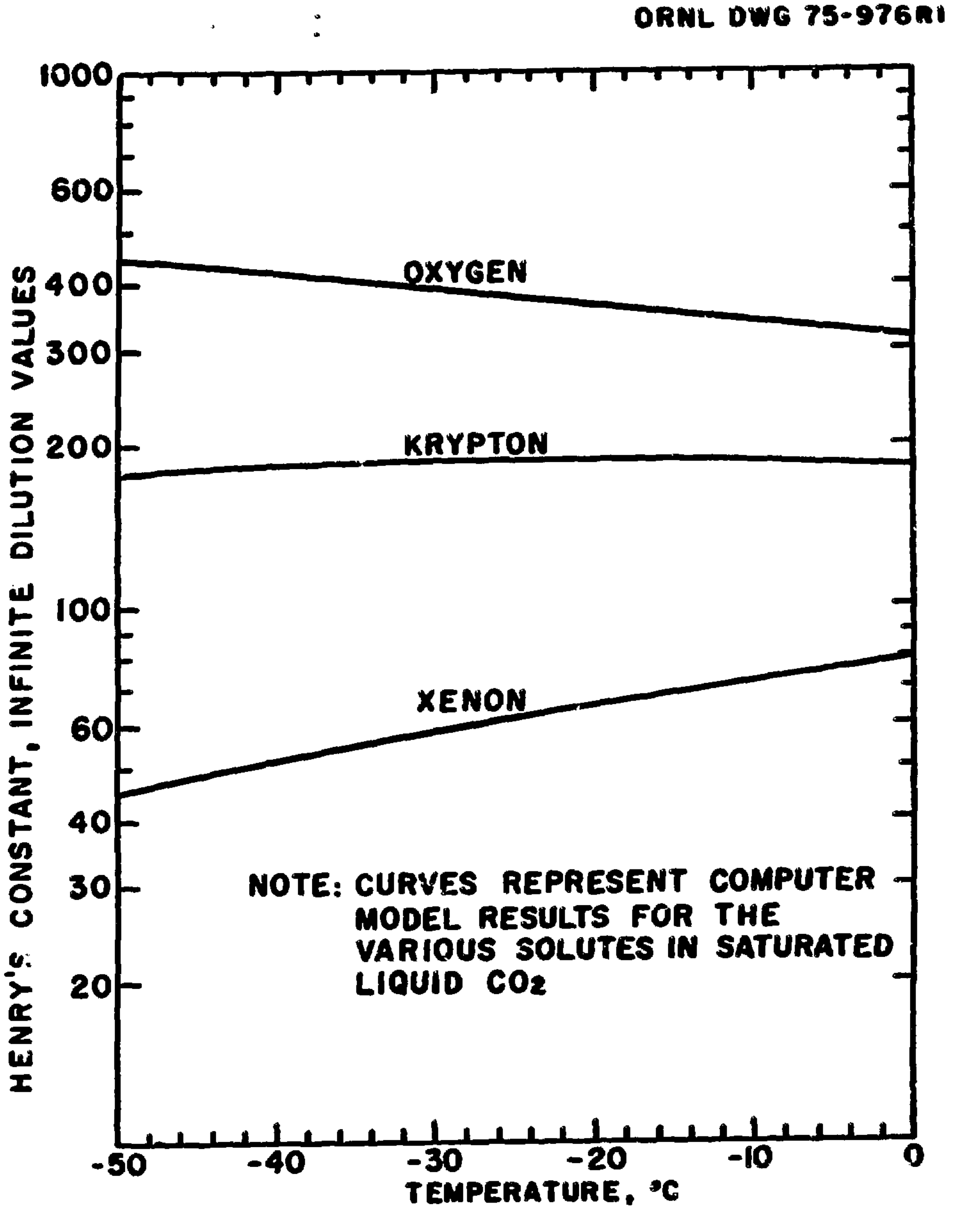

NOTE: CURVES REPRESENT COMPUTER MODEL RESULTS FOR THE VARIOUS SOLUTES IN SATURATED LIQUID CO_2

Fig. 5. Values of Henry's constant for selected solutes as obtained by the computer model.

ORNL DWG 75-978R1

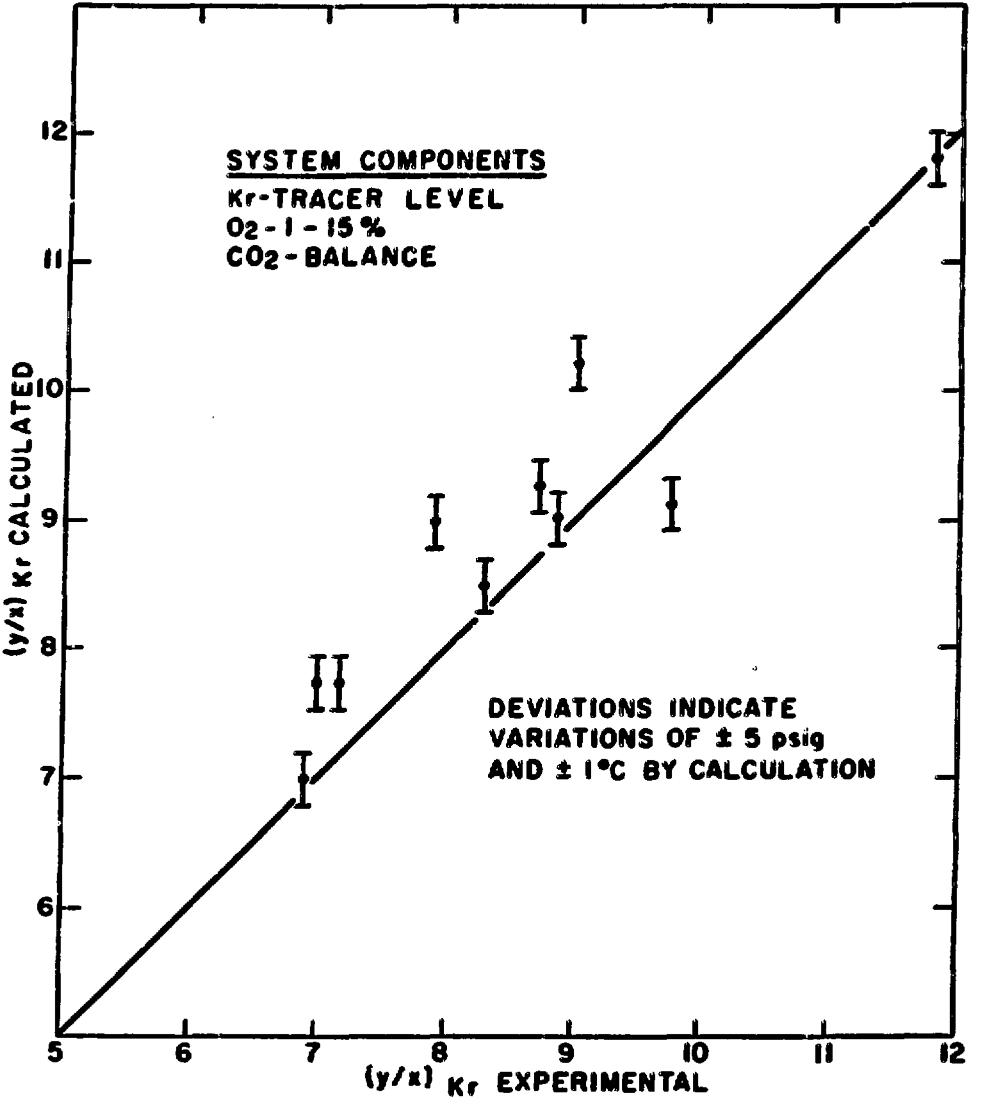

Fig. 6. Comparison of predicted and measured values of $(y/x)_{Kr}$ for the equilibrium experiments.

the value of $(y/x)_{Kr}$ experimental was obtained directly. For each experimental value of P (total pressure) and T (system temperature at the bottom of the absorber), the computer model for the CO_2-Kr-O_2 equilibrium provided a corresponding value of $(y/x)_{Kr}$ calculated. Additionally, the computer model provided a value of y_{O_2} at each P and T for comparison with the measured quantity.

Considering the range of concentrations involved (< 2 mole % O_2 in the liquid and tracer-level krypton), the agreement present in Fig. 6 is remarkably good and would tend to support the data of Notz et al.(3) Thus, for the remaining experiments. the data of Notz et al. are assumed to be valid.

Mass Transfer Experiments

During the mass transfer experiments the EES-ODF was operated in total recycle with approximately 10% light gas (O_2) and tracer-level krypton. The simulated reprocessing off-gas stream was compressed to slightly more than the desired absorption pressure and routed to the bottom of the absorber column. In the absorber, the gas (flowing upward) was contacted with essentially pure liquid CO_2 into which both O_2 and krypton were absorbed as the liquid flowed down the packed section. The solute-laden liquid was then routed to the stripper column where the dissolved gases were desorbed and released into the stripper off-gas stream. The stripper and absorber off-gases were subsequently combined to form feed gas and recycled to the compressor. Liquid leaving the stripper was recycled to the top of the absorber packed section as a continuous flow of solute-free solvent.

For each of the mass transfer experiments, an operating condition was chosen and the entire flow system was allowed time for transients to subside before sampling and data acquisition. Tables 3 and 4 present a portion of the data taken during the mass transfer experiments, and includes data for four experiments (viz., 232, 241, 254, and 539) which were made under pinched conditions that do not reflect the nature of the other mass transfer experiments. These four experiments simply offer a lower bound to operational mass transfer. Some of the values listed in Table 3 were obviously not obtained directly by experiment but, instead, were calculated from more fundamental measurements. The absorber pressure, average absorber temperature, absorber ΔP, and liquid rate are shown as measured. Feed gas rates were dependent on rotameter calibrations, while the O_2 content of the feed gas and overall krypton decontamination factors (DF's) were based on sampling and monitoring.

Data Analysis

During operations only the feed gas stream could be identified with respect to both flow rate (via rotameter) and composition (sampling and analysis). Off-gas streams from the absorber and from the stripper were sampled and analyzed for composition, but their flow rates were not known accurately since flowmeters for these streams were unreliable. Knowledge of the compositions (O_2 and krypton) for these streams, together with the flow rate of the feed gas stream, allows calculation of flow rates for the off-gas streams by assumption of either O_2 or krypton material balances in conjunction with overall stream balances.

Operational experience provides more confidence in the determination of the ^{85}Kr content; therefore, the assumption of a complete krypton balance was made,

Table 3. Summary of absorber conditions during mass transfer experiments

Experiment number	Absorber pressure (psig)	Feed gas rate (scfm)[a]	Feed gas oxygen (%)	Average absorber temp. (°C)	Absorber ΔP (in. H_2O/ft)	Liquid flow rate (gpm)	Overall krypton DF[b]
222	324	5.44	10.35	-20.0	0.364	0.551	357.
232	340	7.09	7.08	-17.4	0.516	0.551	5.
241	254	6.19	9.42	-28.2	0.255	0.495	7.
254	375	7.22	7.79	-12.2	0.619	0.485	3.
309	302	4.65	7.13	-20.1	0.413	0.623	256.
320	308	4.56	6.82	-20.1	0.510	0.720	14039.
330	308	4.57	7.83	-20.4	0.449	0.693	4161.
340	313	4.27	8.99	-20.5	0.473	0.693	7000.
349	310	4.55	9.19	-20.3	0.668	0.749	9687.
359	313	4.73	9.23	-20.8	0.467	0.665	619.
368	321	4.81	12.60	-20.9	0.515	0.623	7236.
378	337	4.99	11.70	-20.0	0.437	0.592	3214.
388	337	4.97	11.64	-20.0	0.449	0.592	3043.
406	304	5.87	20.06	-18.8	0.461	0.554	1215.
416	307	6.21	15.14	-18.3	0.394	0.495	1013.
426	347	5.74	11.93	-20.5	0.443	0.554	153.
436	345	5.39	10.75	-19.3	0.419	0.554	539.
451	325	4.77	11.34	-20.9	0.319	0.416	590.
461	336	4.40	10.47	-19.2	0.323	0.416	2602.
470	333	3.78	8.88	-18.7	0.315	0.416	3075.
480	317	5.23	10.83	-22.2	0.307	0.416	57.
490	323	6.33	5.62	-21.9	0.327	0.416	10.
498	323	3.73	8.45	-18.9	0.303	0.416	5157.
518	405	4.50	7.57	-12.6	0.376	0.416	839.
528	402	3.63	10.05	-11.7	0.376	0.416	4033.
538	409	6.38	7.80	-11.6	0.425	0.416	5.
548	396	5.16	5.93	-12.7	0.399	0.416	17.
558	391	4.67	6.79	-13.2	0.397	0.416	100.
568	407	4.23	6.24	-11.9	0.388	0.416	1106.
578	392	3.49	6.01	-12.17	0.376	0.416	2908.

[a] scfm refers to real CO_2 gas at 70°F and 1 atm.

[b] DF = decontamination factor.

Table 4. Mass transfer values

Experiment number	Overall DF	Column* DF	Krypton HTU (ft)	O_2 balance factor	Absorption factor
222	357	227	0.561	0.93	1.29
232	5	5	1.329	0.94	0.81
241	7	7	0.700	0.94	0.90
254	3	3	3.220	0.97	0.72
309	256	219	0.355	0.94	1.15
320	14039	7757	0.383	0.84	1.43
330	4161	2750	0.339	1.06	1.32
340	7000	4139	0.385	1.02	1.43
348	9687	3866	0.348	1.02	1.45
358	619	471	0.380	1.02	1.23
368	7206	3350	0.374	1.10	1.41
378	3214	1927	0.405	1.02	1.42
388	3043	1887	0.400	0.97	1.40
406	1215	704	0.463	0.99	1.34
416	1013	621	0.464	1.05	1.30
426	153	115	0.506	0.97	1.19
436	539	343	0.493	0.99	1.33
451	590	354	0.430	0.93	1.27
461	2602	1267	0.418	0.94	1.42
470	3075	1358	0.482	0.95	1.55
480	87	72	0.345	0.99	1.07
490	10	10	0.588	0.92	0.92
498	5157	2119	0.441	1.08	1.58
518	839	642	0.400	0.98	1.26
528	4038	2455	0.378	0.92	1.40
538	5	6	1.720	0.98	0.87
548	17	18	0.816	0.99	1.02
558	100	96	0.479	0.96	1.13
568	1100	830	0.448	0.98	1.32
578	2908	1543	0.419	0.94	1.41

*Column DF's are calculated values which pertain to conditions at the top and bottom of the packing itself.

and the inaccuracies involved in flow rate, O_2 content, and krypton content have been combined into the oxygen balance factor noted in Table 4.

The overall krypton DF as presented in Table 3 is calculated from the krypton present in the feed gas and absorber off-gas streams as follows:

$$\text{Overall DF} = \frac{\text{Amount of Kr in feed gas}}{\text{Amount of Kr in absorber off-gas}} \quad . \tag{2}$$

Calculations of HTU's for krypton are based on the following simple and classical equations:(8)

$$\text{HTU} = Z/\text{NTU}, \tag{3}$$

$$\text{NTU} = \frac{y_o - y_i}{(y^* - y)_{lm}} \quad , \tag{4}$$

$$(y^* - y)_{lm} = \frac{(y_o{}^* - y_o) - (y_i{}^* - y_i)}{\ln \dfrac{y_o{}^* - y_o}{y_i{}^* - y_i}} \quad , \tag{5}$$

where

HTU = height of transfer unit, ft,

Z = column packing height, ft,

NTU = number of transfer units,

y_i = inlet gas composition,

y_o = outlet gas composition.

Asterisked quantities (e.g., $y_i{}^*$) indicate phase compositions that are in equilibrium with corresponding compositions in the adjacent phase. All compositions refer to krypton; Z = 8.24 ft and $y_o{}^* = 0$. Values of HTU calculated by using Eq. (3) are presented in Table 4. Figure 7 illustrates the variation of the packing HTU with column DF. Figure 8 shows the variation of column DF with absorption factor.

Discussion

As necessary for clarity, certain details have been included with the experimental and analytical procedures already presented. A more complete discussion of the present work is presented in Reference 9. Earlier campaigns and reports concerning the EES-ODF have noted the experimental nature of the facility. The presentation of details indicate clearly one aspect of this facility. The facility, by design, is intended to provide development data as opposed to demonstration-type information. Development data collected relate specifically to krypton absorption by liquid CO_2. Subsequent work will be concerned with other operations of importance in the KALC process, such as fractionation of lighter gases that are coabsorbed with krypton or complete stripping of all

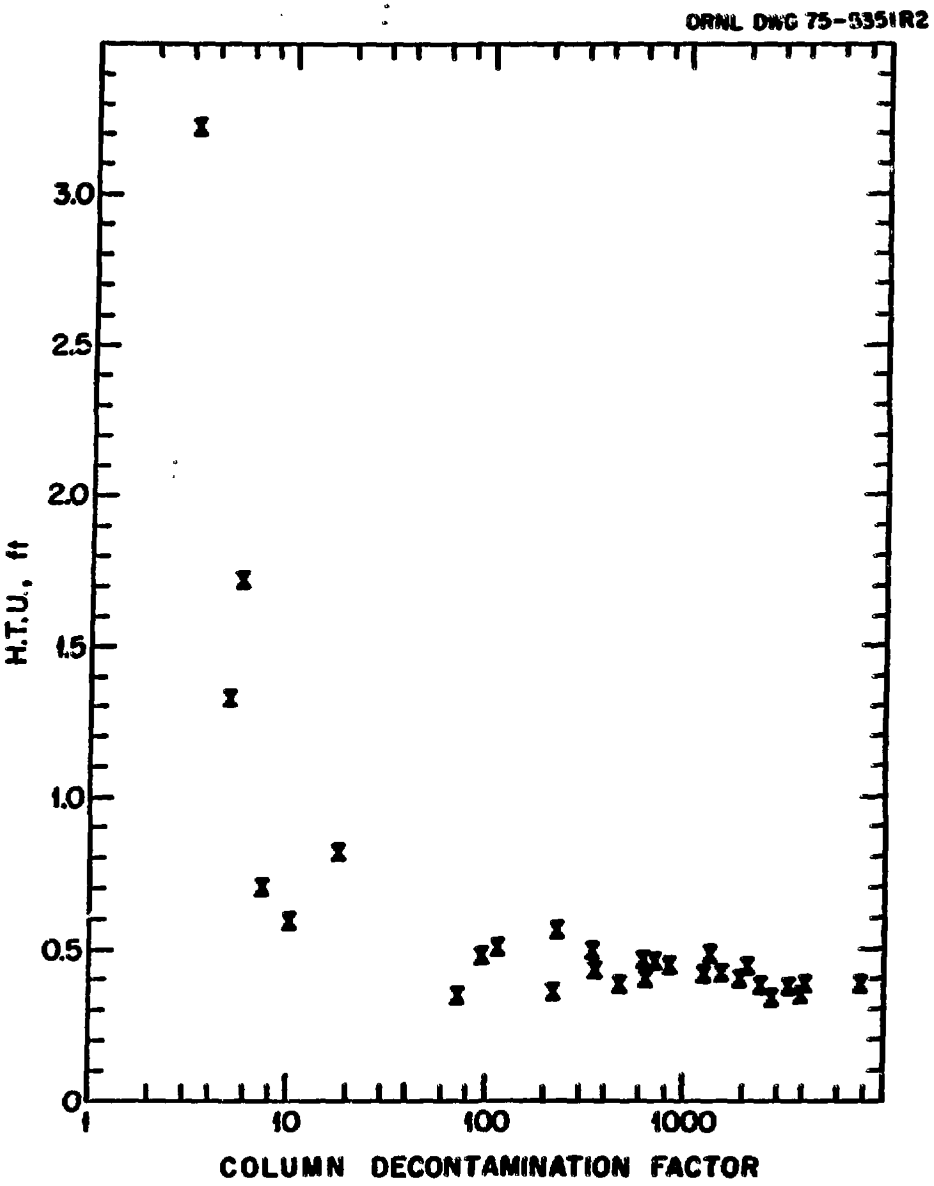

Fig. 9. HTU values for Campaign II experiments.

7

ORNL DWG 75-5352 R2

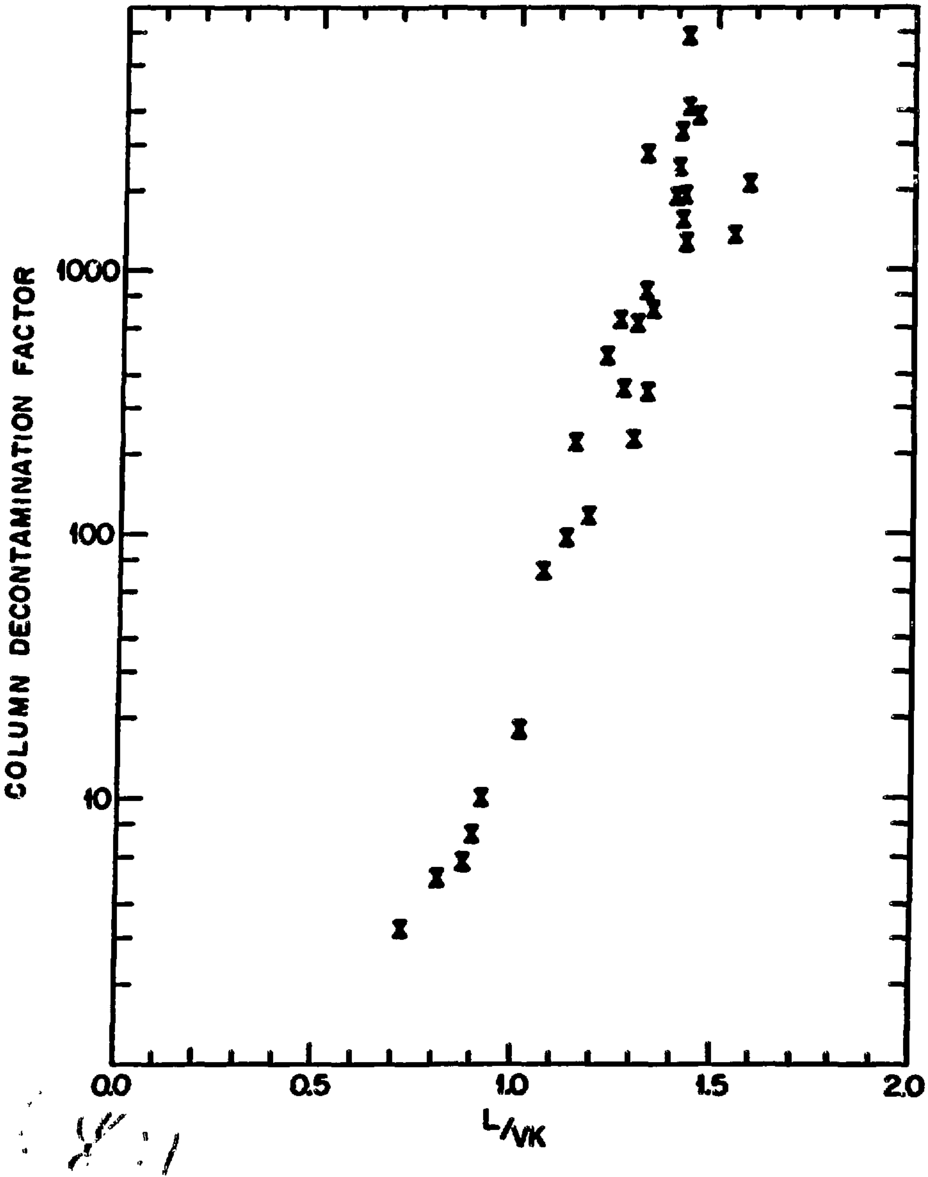

Fig. 8. Decontamination factors vs absorption factors for Campaign II experiments.

dissolved light gases. Each of these operations is important in the total development of the KALC process, but the EES-ODF is not designed to study all operations simultaneously. The facility is not a prototype KALC system. Rather, it represents an engineering-scale system designed to study individual operations of the KALC process under experimental conditions as closely similar to those expected in an overall process as possible.

Many features of the EES-ODF will undoubtedly have counterparts in a conceptual or subsequent design of the KALC system; however, such features will require technical review for operability, compatibility, and desirability before scale-up to the commercial or semicommercial system can occur.

The curve shown in Fig. 2 is of the form typically presented(10) as the "generalized" flooding curve except that the usual parameters, a_p/ϵ^3, in the ordinate grouping for the particular packing characteristics have been omitted. (Generally, a_p is the total area of packing (ft^2/ft^3 bed), and ϵ is the void fraction in dry packing.) Moreover, the curve in Fig. 2 only resembles the generalized curve and does not correspond exactly in shape. At any value of the abscissa grouping, the ratio a_p/ϵ^3 (i.e., the packing factor) can be evaluated by calculating the ratio of the generalized curve ordinate grouping to that of Fig. 2. For example, at a value of the abscissa grouping of unity (near the center of both flooding curves), the packing factor is calculated to be 215 by this method. Hence, in the instance described, the packing of Fig. 2 may be compared to other types as follows:

Packing type	a_p/ϵ^3	Relative factor
1/2-in. ceramic Raschig rings	428	1.99
5/8-in. polypropylene Pall rings	158	0.73
1/2-in. ceramic Berl saddles	596	2.77
1/2-in. ceramic Intalox saddles	400	1.86
Goodloe wire mesh packing	215	1.00

The relative factors presented above do not necessarily indicate a packing quality or utility higher or lower than the packing used. Two important performance considerations here are throughput (or capacity) and HTU.

Figure 2 presents evidence that the flooding characteristics of the packing for the 1-1/2-in.- and 3-in.-diam columns are essentially identical for the conditions investigated. Whether identical results will also be obtained in larger-diameter columns is not known. The effect of packing density has not really been determined for the wire mesh packing investigated.

It should be noted that in the event that diameter greatly influences the flooding (and therefore the capacity) in large columns, the use of other "dumped" packings would not circumvent this problem. In fact, the relative size of dumped packing to column diameter may be more difficult to handle for scale-up purposes than considerations of the density of mesh packing.

From the standpoint of capacity and within the available time for testing, it appears likely that the wire mesh will provide a reasonable basis for scale-up without undue compromise in mass transfer performance. Also, this material will probably be at least comparable, with regard to capacity, to other commercially available packings.

The question of mass transfer performance is another important consideration when selecting a packing material. The present work concerns only absorption in the 1-1/2-in. EES-ODF column. Figure 7 shows that for reasonable values of operational parameters a value of 0.4 to 0.5 ft for HTU results. A number of considerations relating to the accuracy of the calculational procedures will be discussed later. Of question here is whether the HTU value will vary appreciably with column diameter. Obviously, the question cannot be answered from the present absorption experiments alone.

Most of the important considerations in equilibrium operations have been discussed previously. At the time the experiments were performed, valid questions existed as to (1) the importance of the equilibrium data accuracy, and (2) the effect of uncertainties in the equilibrium ratios (y/x). Certainly, the data of Notz et al. do exhibit an internal consistency over a relatively large range of temperatures, and all of their data are reported at essentially infinite dilution. Correlation techniques were used by Mobley to test the apparent consistency with other solutes in liquid CO_2. The net result of the equilibrium operations, together with the finding of Mobley, is that, while the data of Notz et al.[3] are definitely more nearly accurate, a margin of uncertainty regarding absolute accuracy remains.

Just how important it is that the Kr-CO_2 equilibrium values are known to within a given range, say ± 10%, is not clear. Based on HTU values calculated with Eq. (3), a qualitative relation exists between HTU and K as follows:

$$HTU_2 = HTU_1\left[\frac{K_2}{K_1}\right]^{-3} . \qquad (6)$$

Consequently, a 10% variation in K (i.e., ± 5%) would result in a ± 15% uncertainty in HTU. Such an uncertainty in HTU would not be unacceptable *per se*; however, the true range of uncertainty would undoubtedly be larger since other factors are known to contribute.

Figure 6 indicates a slightly lower experimental value of $(y/x)_{Kr}$ than one would predict using the data of Notz et al. Mobley's findings via correlations also indicate a slightly lower value and thus tend to fall more in line with other solute behavior in liquid CO_2. Both the equilibrium operations considered here and elements of the correlation work exhibit uncertainties, so that it cannot be stated absolutely that the data of Notz et al. are in error. Finally, although the equilibrium experiments were tedious and time-consuming, perhaps more confidence could be placed in the results if additional experiments had been conducted. At the present time, however, there appears to be no compelling reason why the data of Notz et al. should not be accepted.

During the present mass transfer experiments, the independent variable of primary importance was the absorption column liquid-to-vapor flow ratio (L/V). Ranges for this and other important variables are summarized as follows:

Variable	Range
Pressure, psig	254 to 409
Temperature, °C	-28.2 to -11.6
Feed O_2 concentration, vol %	5.93 to 20.06
Liquid-to-vapor ratio	
Overall values	4.94 to 12.82
Column only	5.04 to 12.88

It should be recognized that a 1:1 correspondence does not exist for the above variables over their ranges. That is, the experiment with the highest pressure is not necessarily the experiment with the highest L/V, etc. However, the variables are not totally independent, and a careful review of all variables presented throughout this report is necessary for an appreciation of the nature of the absorption process.

An important experimental observation is that variables do behave relative to one another as would be expected based on thermodynamic and chemical engineering principles. In short, no surprises were found. Of equal importance was the considerable operational experience gained, which will be of use in subsequent campaigns and for scale-up design analyses. In some ways, the study of absorption may be the least difficult of the studies required (viz., absorption, fractionation, and stripping). However, there are certain similarities among the three studies, and the discussion presented in this report regarding absorption should be applied to future plans for fractionation and stripping experiments.

The few results that indicate appreciably higher values of HTU than 0.4 ft (see Fig. 7) were obtained in essentially pinched experiments, where the HTU equation is erroneously attributing all the mass transfer to the entire packing length instead of to the shorter, effective length. The result is a higher apparent HTU value, and this phenomenon is not unexpected. The fact that Fig. 8 shows a rather sharp increase in DF as the value of the "absorption factor," L/VK, exceeds unity is indicative of (1) more than just a "few" stages in the absorber, and (2) the "correct" choice of experimental $Kr-CO_2$ equilibrium data. If only a few stages were present, it would be expected that DF would not increase as rapidly with L/VK. If the data of Beaujean et al.[2] were correct (or if the data of Notz et al. were grossly in error), the "inflection" of the DF curve of Fig. 8 would not necessarily be at $L/VK = 1$. Of course, the value of L/V used in L/VK could be in error; nevertheless, it is doubtful that the general error associated with L/V would exactly compensate for a corresponding uncertainty in K. Further, since DF is essentially a measured quantity, the ordinate of Fig. 8 can be expected to be indicative of the true situation as far as curve shape is concerned.

Conclusions

The present work has provided a wealth of operating experience on which subsequent operations can realistically be based. Sampling and analytical techniques appear to be valid and provide a relatively quantitative measurement of composition. However, the absolute accuracy of composition measurements can be evaluated only with additional experimentation.

Flooding performance of the wire mesh packing is reasonably well correlated for the conditions and equipment studied. The krypton equilibrium data of Notz et al.(3) appear to be sufficiently accurate for experimental purposes of the EES-ODF. For process decontamination factors on the order of 1000, a value of 0.5 ft for the krypton absorption HTU seems realistic and, within the range of the experiments conducted, does not vary for reasonable absorption conditions.

References

1. R. W. Glass, H. W. R. Beaujean, H. D. Cochran, Jr., P. A. Haas, D. M. Levins, and W. M. Woods, "Development of the Krypton Absorption in Liquid Carbon Dioxide (KALC) Process for HTGR Off-Gas Reprocessing," *Proceedings of the 13th AEC Air Cleaning Conference*, August 12-15, 1974, pp. 232-245.

2. H. W. R. Beaujean et al., "Off-Gas Treatment and Krypton Disposal in HTGR-Fuel Element Reprocessing," presented at the Symposium on the Management of Radioactive Wastes from Fuel Reprocessing, Paris, France, November 27 - December 1, 1972.

3. K. J. Notz, A. B. Meservey, and R. D. Ackley, "The Solubility of Krypton and Xenon in Liquid CO$_2$," Trans. Am. Nucl. Soc. 17, 318-19 (1973).

4. M. J. Stephenson, et al., "Absorption Process for Removing Krypton from the Off-Gas of an LMFBR Fuel Reprocessing Plant," *Proceedings of the 13th AEC Air Cleaning Conference*, August 12-15, 1974, pp. 263-275.

5. R. M. Mobley, "Calculations for the Separation of Radioactive Krypton from the Off-Gas from the Reprocessing of High Temperature Gas-Cooled Reactor Fuel Elements," M.S. Thesis, Department of Chemical Engineering, Clemson University, Clemson, S.C., August 1973.

6. D. M. Levins, R. W. Glass, M. M. Chiles, and D. J. Inman, *Monitoring and Analysis of Process Streams in a Krypton-85 Off-Gas Decontamination System*, ORNL/TM-4923 (July 1975).

7. R. W. Glass, T. M. Gilliam, and V. L. Fowler, *An Empirical Model for Calculating Vapor-Liquid Equilibrium and Associated Phase Enthalpy for the CO$_2$-O$_2$-Kr-Xe System for Application to the KALC Process*, ORNL/TM-4947 (January 1976).

8. A. S. Faust et al., *Principles of Unit Operations*, p. 278, Wiley, New York, 1960.

9. R. W. Glass, et al., *Krypton Absorption in Liquid CO$_2$ (KALC): Campaign II in the Experimental Engineering Section Off-Gas Decontamination Facility*, ORNL/TM-5095, 2 (February 1979.

10. R. H. Perry and C. H. Chilton (eds.), *Chemical Engineers' Handbook*, 5th ed., p. 18-22, McGraw-Hill, New York, 1973.